J Mater Sci (2010) 45:4665–4671
DOI 10.1007/s10853-010-4675-1

ULTRAFINE GRAINED MATERIALS

Texture and microstructure evolution in ultrafine-grained AZ31 processed by EX-ECAP

M. Janeček · S. Yi · R. Král · J. Vrátná · K. U. Kainer

Received: 12 February 2010 / Accepted: 28 May 2010 / Published online: 22 June 2010

Abstract Extruded AZ31 alloy was processed by equal channel angular pressing (ECAP) up to 12 passes at 180 °C following route B_c, i.e. rotating the sample 90° between individual passes. Microstructure evolution was investigated using EBSD and TEM, as a function of strain imposed by ECAP. The first ECAP pass resulted in the formation of a new texture component which relates to the bimodal grain structure observed in this specimen. The grains larger than 10 μm show the orientation changes corresponding to the ECAP shear, which is characterised by the rotation of the basal poles by approximately 40° from the initial orientation. The fine grains with the average size of 1 μm maintain the initial orientation. The character of the bimodal grain structure and the distinct texture components between large and small grains remained unchanged up to 4 ECAP passes. Further ECAP pressing to 8 and 12 passes leads to a grain refinement through the whole sample volume and the orientation changes of all grains corresponding to the ECAP shear.

Introduction

Magnesium alloys are gaining a renewed interest due to their high specific strength, being potentially a promising material for structural components in automotive and aerospace industries. Nevertheless the applications of Mg alloys are still limited, because of problems associated with limited ductility and relatively low strength. The limited ductility is a consequence of the lack of independent slip systems and the large difference in values of the critical resolved shear stress in the potential slip systems. Moreover, the occurrence of strong deformation textures and stress anisotropy in magnesium alloys reduces significantly the variety of possible industrial applications [1].

The properties of magnesium alloys can be improved by refining the grain size to the submicrocrystalline (grain sizes in the range of 100–1000 nm) or even nanocrystalline level (grain sizes smaller than 100 nm) [2, 3]. A variety of new techniques have been proposed for the production of the ultrafine-grained (UFG) structure in materials, e.g. the high-pressure torsion [4] or accumulative roll-bonding [5]. Equal channel angular pressing (ECAP), first reported by Segal [6], became a very popular technique due to its versatility and scalability beside its effectiveness in producing UFG structure. ECAP activates the prismatic and pyramidal slip systems and the resulting texture re-activates the basal slip [7].

Multiple processing of samples by ECAP leads to changes in properties and microstructure. The dependence on the number of passes is typically non-monotonous, exhibiting an extreme value after 3–5 passes through the die [8].

The aim of this study is to investigate the microstructure and the texture evolution resulting from gradual material processing by ECAP up to 12 passes and to correlate microstructure changes with mechanical properties of the commercial magnesium alloy AZ31.

Experimental procedures

Magnesium AZ31 alloy was processed by ECAP resulting in a maximum equivalent strain of 12 (1, 2, 4, 8 and 12

M. Janeček (✉) · R. Král · J. Vrátná
Department of Physics of Materials, Charles University, Prague, Czech Republic
e-mail: janecek@met.mff.cuni.cz

S. Yi · K. U. Kainer
Magnesium Innovation Centre, GKSS-Research Centre, Geesthacht, Germany

passes). Prior to ECAP, the specimens were extruded at 350 °C with extrusion ratio of 22. The ECAP die was equipped with an ejector that allows to push the sample out of the die immediately after its pressing by a plunger from the feed-in channel to the exit channel. The main advantage of the ejector is the shorter time the sample is exposed to the operating temperature of the ECAP process, thus avoiding the possible microstructural changes. ECAP pressing was performed at 180 °C following route B_c, i.e. rotating the sample 90° between the individual passes, at the speed of 50 mm/min and molybdenum disulphide grease was used as a lubricant. The angle Θ between two intersecting channels and the corner angle Ψ were 90° and 0°, respectively. Both channels have a square cross section of 10 mm × 10 mm.

The texture of extruded and the ECAPed samples were measured by electron backscatter diffraction (EBSD). Samples for EBSD measurements were cut from individual specimens after ECAP from the plane perpendicular to the pressing direction (plane X) and prepared by electrochemical polishing using Struers-AC2 electrolyte at −15 °C and 33 V for 90 s.

Transmission electron microscopy (TEM) investigations were performed with a Jeol 2000FX electron microscope operated at 200 kV. Thin foils for TEM were first mechanically polished and finally ion-polished using a Precision Ion Polishing System (PIPS) at 4 kV.

Tensile tests were performed using a screw-driven Instron 5882 machine at the initial strain rate of 10^{-4} s^{-1} at room temperature. Flat specimens for tensile tests were machined from ECAP billets with the lengthwise axis parallel to *X*-direction and the plane of the specimen perpendicular to the *Y*-direction. The geometry of the tensile specimens corresponds to a gage length of 40 mm, the thickness and width were 1 and 6 mm, respectively.

Results

Microstructure and texture evolution

Figure 1 shows the microstructure and texture of the extruded AZ31 alloy. The EBSD inverse pole figure map is in the extrusion direction (ED).

The microstructure of the initial extruded bar (0P) consists of large grains of 50–100 μm mixed with relatively fine grains of 2–5 μm. Most grains have their crystallographic *c*-axis perpendicular to the extrusion direction (ED), i.e. ⟨10.0⟩ axes parallel to the ED, which is typically found after extrusion of Mg alloys [9].

Figure 2 presents the microstructure and texture of the sample after 1 ECAP pass (1P). EBSD measurements were carried out at the mid-part of the cross-section of the billet.

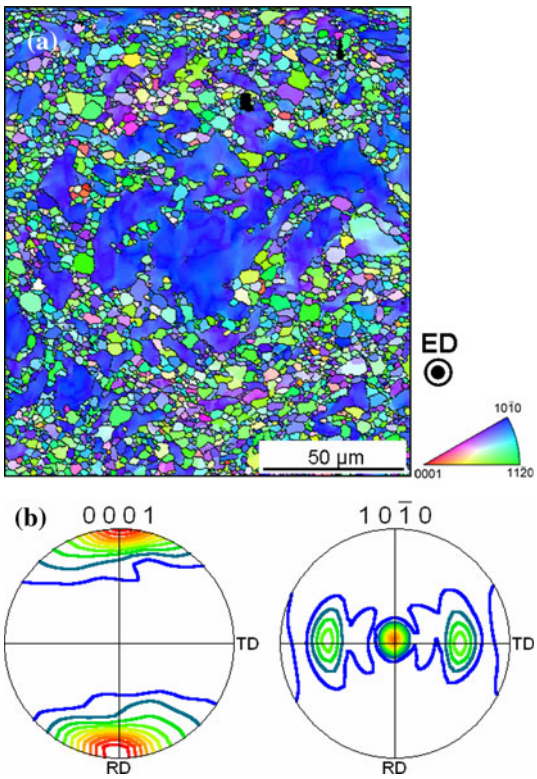

Fig. 1 **a** EBSD orientation map and **b** recalculated pole figures of the extruded bar (0P), measured at the cross-section transverse to the extrusion direction (contour level = 1, 2, … 10)

Sample coordinate system, i.e. *X*–*Y*–*Z* directions, which is used for representing the texture are illustrated in Fig. 2d. As shown in Fig. 2a, the bimodal distribution of grain sizes is still observed in the 1P sample. A new texture component which corresponds to the basal poles rotated about 40° from the initial orientation towards the pressing direction is visible in the 1P sample, Fig. 2b. The mentioned orientation change, however, is observed mainly in large grains (grain size > 10 μm). Figure 2c presents the (0001) pole figure of grains smaller than 3 μm in the 1P sample. The intensity of the tilted basal poles is rather weak compared to the pole figure constructed using all grains. Moreover, the small grains (<3 μm) with the tilted basal pole are found mainly in neighbouring areas around large grains.

These results regarding distinct textures depending on the grain sizes indicate that the shear strain by the first ECAP pass is mainly accommodated within the large grains. It corresponds well to the fact that larger grains are deformed by lower energy comparing to the small grains, e.g. Hall–Petch relation. The discontinuity of material flow caused by the inhomogeneous deformation seems to be compensated by the occurrence of the dynamic recrystallisation in the vicinity of grain boundaries of large grains, such that the sample could be deformed without failure.

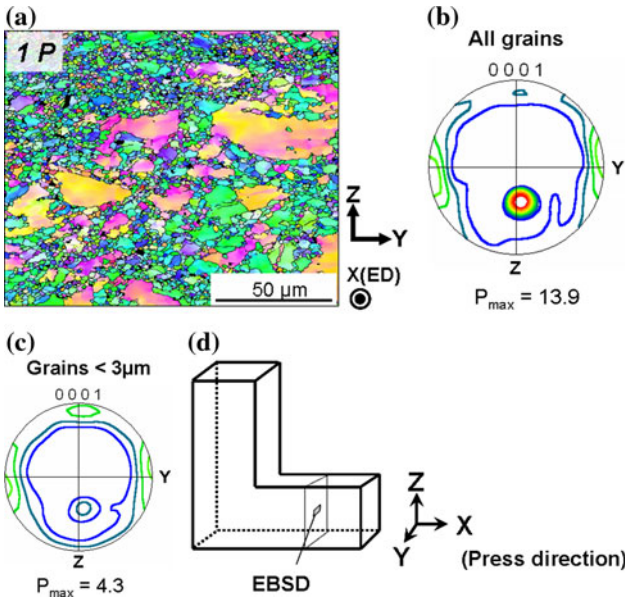

Fig. 2 **a** EBSD orientation map of the sample after 1 ECAP pass, **b** (0001) pole figure calculated using all grains, **c** (0001) pole figure of grains smaller than 3 μm and **d** the scheme of the geometry of specimens for EBSD measurements (contour level = 1, 2, … 10)

Microstructural features of the sample after 2 ECAP passes (not shown here) are very similar to those after 1 ECAP pass, i.e. the bimodal distribution of grain sizes and the orientation change in large grains remain almost unchanged.

The amount of large grains decreases significantly after 4 ECAP passes (4P), and their size becomes smaller when compared to the initial and the 1P samples (see Fig. 3). As shown in the Fig. 3a with dashed circles, the fine grains are visible at the mantel of large grains. Differently to the 1P sample, the fine grains (<3 μm) have mainly the orientation of the rotated basal poles in the 4P sample, Fig. 3c. It is clear that the texture heterogeneity depending on the grain size disappears after 4 ECAP passes, compared pole figures evaluated from the whole area of the EBSD measurement to that from fine grains, Fig. 3b and c, respectively.

The microstructure and the texture of the sample after 12 ECAP passes (12P) are presented in Fig. 4. The 12P sample shows the homogeneous distribution of fine almost equiaxed grains, i.e. no large grains are visible. Figure 4a shows grain agglomerates, having different colours, distributed along a diagonal line. This indicates the heterogeneity in texture depending on the locations. This texture inhomogeneity can be understood as a result of non-uniform deformation along the ECAP billet after multiple passes [10]. Though the heterogeneous texture is visible, the fraction of the grains relating to the inhomogeneity is small such that the main texture component is found at the rotated basal pole, Fig. 4b.

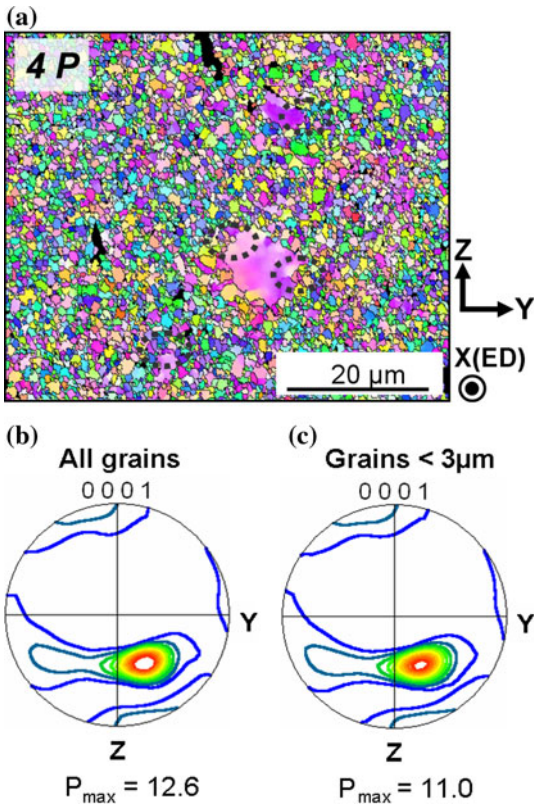

Fig. 3 **a** EBSD orientation map of the sample after 4 ECAP passes, **b** (0001) pole figure of all grains and **c** grains smaller than 3 μm (contour level = 1, 2, … 10)

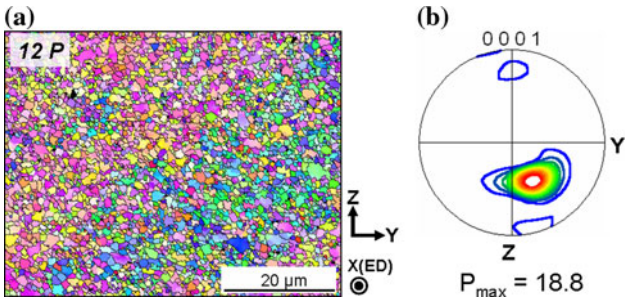

Fig. 4 **a** EBSD orientation map and **b** (0001) pole figure of the sample after 12 ECAP passes (contour level = 1, 2, … 15)

Figure 5 displays size distributions of fine grains (<10 μm) after different ECAP passes. The variation in the area fraction of large grains (>10 μm) is shown in Table 1. Grains smaller than 3 μm present in the extruded sample (0P) become finer (~1 μm) after the first ECAP pass. In subsequent ECAP passes no significant change in the size distribution in the range of the relatively fine grains is observed, while the area fraction of grains larger than 10 μm decreases gradually with ECAP passes, see Table 1.

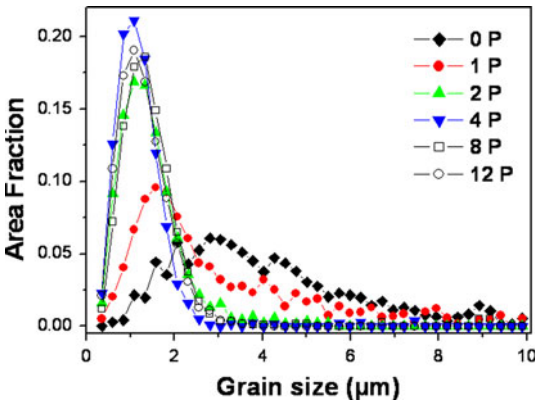

Fig. 5 Grain size distributions within the range up to 10 μm and the area fraction of the grains larger than 10 μm, as a function of the ECAP pass number

Table 1 Area fraction of large grains as a function of ECAP pass number

ECAP passes	Area fraction of grains > 10 μm (from EBSD map)
0	0.18
1	0.18
2	0.08
4	0.03
8	None

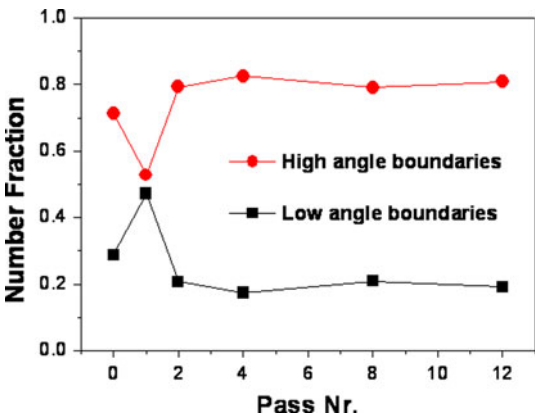

Fig. 6 Variation of fraction of the HAB and LAB as a function of the ECAP pass number

The variation in the fraction of low (misorientation angle $< 15°$, LAB)- and high-angle boundaries (misorientation angle $> 15°$, HAB) as a function of the ECAP pass number is shown in Fig. 6. The LAB fraction increases after 1 ECAP pass to $\sim 50\%$, and is significantly reduced ($\sim 20\%$) after two ECAP passes and remains almost unchanged as the number of passes increases above 2. This stabilisation of the HAB formed by 2 ECAP passes indicates that the dislocations generated by ECAP did not reach the level necessary for the formation of dislocation cell-structure and further development of HAB. Since the ECAP in this study was carried out at moderate temperature, the dislocations annihilation process by the dynamic recovery occurred fast enough such that the grains could not be further refined after 2 ECAP passes.

Microstructure observations by transmission electron microscopy

The bimodal character of the microstructure of the as-extruded specimen is shown in Fig. 7. In Fig. 7a, the zone containing small grains of the average size of 2–3 μm is shown. In several grains twins are clearly visible. Electron diffraction analysis confirmed the (0001) basal texture of individual grains. The contrast of individual grains on this micrograph with typical low-angle grain boundaries confirms the analysis of diffraction patterns. In Fig. 7b, a region of a large grain is displayed. It is a typical heavily deformed structure containing the high density of dislocations.

TEM micrograph showing the microstructure of the specimen after 1P is shown in Fig. 8. One pass of ECAP pressing did not change the bimodal character of the microstructure. In Fig. 8a, a fine grain zone is shown. The grain size is only slightly smaller as compared to the as-extruded specimen. The main difference between these two specimens is in the character of grain boundaries. Many high-angle grain boundaries with typical fringe band contrast, confirming their almost equilibrium state, are seen in this micrograph. On the other hand, several grain boundaries remained in a non-equilibrium state with diffuse fuzzy contrast and many dislocations lying in a grain boundary plane were also observed. Moreover, several zones containing a high density of tangled dislocations with no or only exceptional signs of substructure formation were found in this specimen. One example is shown in the micrograph in Fig. 8b.

TEM observations confirm the process of microstructure evolution and its fragmentation. In particular, the fine grains were refined only slightly during subsequent ECAP pressing. On the other hand, large grain zones were continuously refined and in the specimen after 8P only fine grains of the average grain size in the submicrometer range were observed. The typical microstructure of the specimen after 8P of ECAP is displayed in Fig. 9. Equiaxed grains of average size of 800 nm with a significantly lower density of dislocations and equilibrium grains boundaries are clearly seen in this micrograph. A few newly recrystallized grains of the size of approximately 500 nm and smaller with no dislocations and sharp boundaries were also found in the microstructure. One example is marked in the micrograph. Further ECAP pressing resulted in slight microstructure

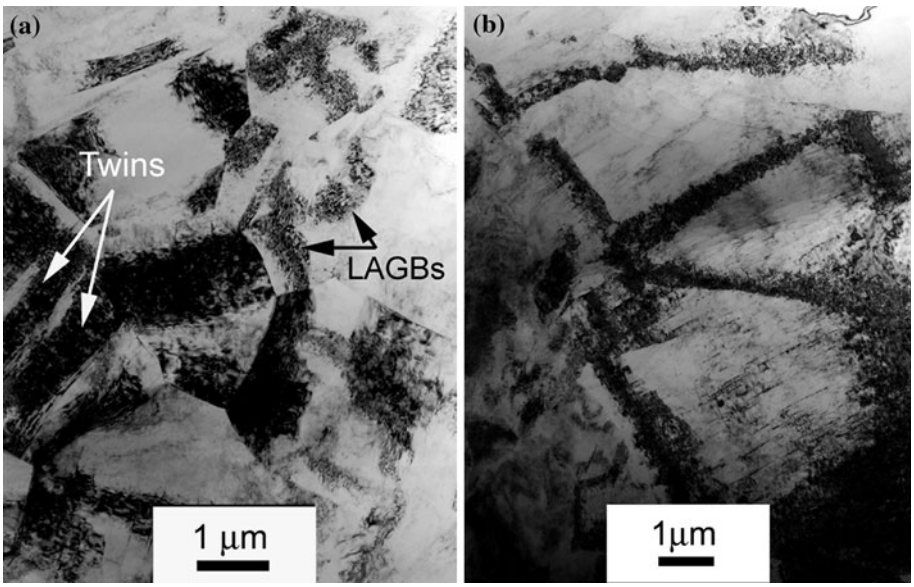

Fig. 7 TEM micrograph of the extruded AZ31 alloy **a** zone of fine grains, **b** coarse grain

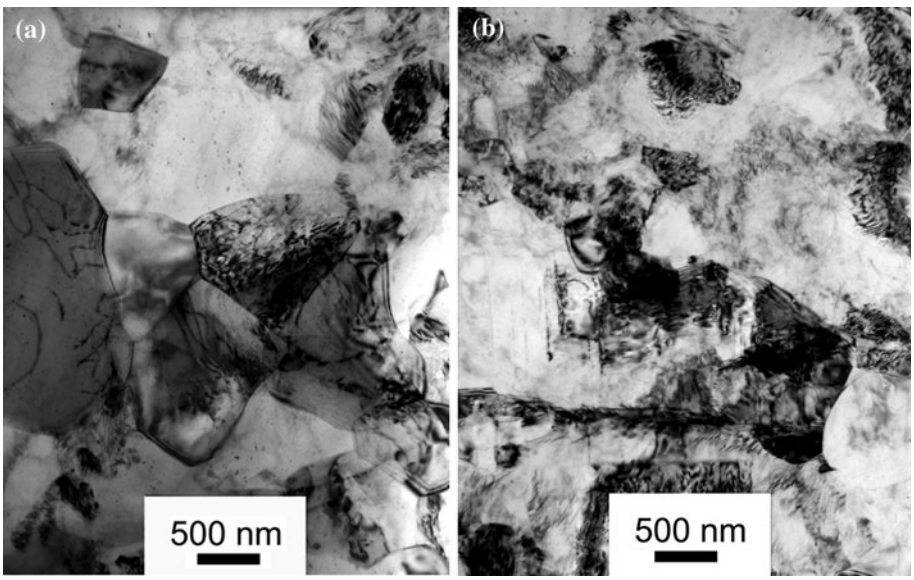

Fig. 8 TEM micrograph of the specimen after 1P of ECAP **a** zone of fine grains, **b** coarse grain

changes only. No new typical features were observed in the specimen after 12P.

Mechanical properties

The stress–strain curves of AZ31 EX-ECAP specimens after various numbers of ECAP passes have been published and analysed in detail elsewhere [8]. Here, we concentrate on the evolution of characteristic stresses with strain due to ECAP. The dependence of the yield stress at 0.2% offset strain on the number of ECAP passes is presented in Fig. 10. Three regions can be distinguished in this dependence: (i) regions 0P–2P with a moderate increase of the yield stress, (ii) regions 8P–12P with a moderate decrease of the yield stress, and (iii) a transient region with a sharp decrease of the yield stress at 2P–8P. The error bars in Fig. 10 combine the errors in sample cross-section and the uncertainty in evaluation the yield point from the stress versus total strain curve.

Discussion

The development of the new texture component characterised by the rotated basal poles towards the pressing direction in the 1P sample, cf. Fig. 2b, is caused by the shear strain imposed by ECAP [11]. The formation of fine grains near grain boundaries of large grains in the Fig. 3a indicates that the refinement of the large grains occurs gradually with increasing number of ECAP passes by

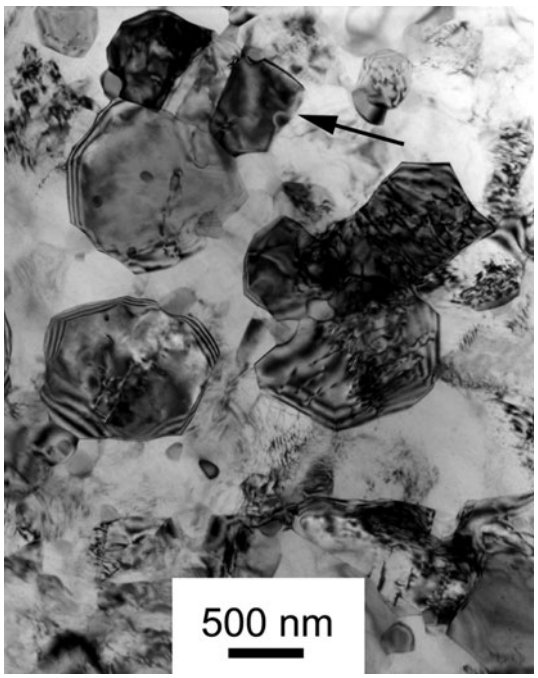

Fig. 9 TEM micrograph of the specimen after 8P of ECAP

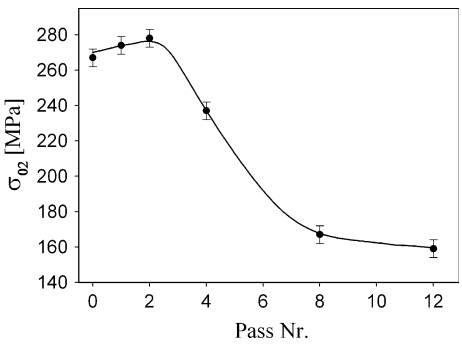

Fig. 10 Dependence of the yield stress on the number of ECAP passes *N*

dynamic rotation recrystallisation mechanism suggested by Ion et al. [12]. The magnitude of rotation of the initial texture (40°) is slightly smaller in this study than in [13], where the minimum rotation angle observed was 45°.

The existence of the transient region in the dependence of yield stress on the number of ECAP passes, see Fig. 10, corresponds well to measurements of Serebryany et al. [13] where the authors reported the decrease of the yield stress from 244 MPa in an initial sample to 182 MPa in a 4P ECAP sample. The difference in the values of yield stress from this study can be ascribed to different initial textures before the ECAP process [14]. This effect can reach up to 20% as has been shown by Al-Maharbi et al. [15]. Nevertheless, contrary to the conclusion in [13, 15], we assume that the yield stress is also, according to the Taylor relation, affected by the dislocation density and its evolution with strain due to ECAP. Our measurements of dislocation densities by positron annihilation spectroscopy have shown substantial differences in dislocation densities in individual samples after ECAP [16]. The dislocation density was found to increase from about 1.6×10^{12} m^{-2} in the initial state to 2.7×10^{12} m^{-2} at 2P. Further straining resulted in a continuous decline of the dislocation density up to $\sim 1.6 \times 10^{12}$ m^{-2} at 12P. The changes of the flow stress with strain (number of ECAP passes) may be explained by a combined effect of both texture and dislocation density variations in individual specimens after the ECAP.

Summary and conclusions

The microstructure and texture evolution in commercial AZ31 alloy processed by EX-ECAP was studied. The results may be summarised as follows:

- The first pass (1P) of ECAP results in the formation of a new texture component inclined by about 40° relatively to the initial texture,
- The bimodal character of the microstructure remains unchanged up to 4P of ECAP.
- Further ECAP pressing (8 and 12P) results in a completely refined microstructure.
- Local TEM observations confirm EBSD results in individual specimens after different number of ECAP passes.

We can conclude that the refinement of large grains occurs gradually with increasing ECAP passes by dynamic rotation recrystallization mechanism.

Acknowledgement This study was financially supported by GACR under the Grant 106/09/0482. J. Vrátná acknowledges financial support by GAUK under the Grant 9594/2009 and under the Grant SVV-2010-261303. Partial financial support by the Ministry of Education and Youth of the CR under the Grant MEB100914 is also gratefully acknowledged.

References

1. Agnew SR, Horton JA, Lillo TM, Brown DW (2004) Scripta Mater 50:377
2. Estrin Y, Yi SB, Brokmeier HG, Zuberova Z, Yoon SC, Kim HS, Hellmig RJ (1998) Int J Mater Res 99:50
3. Figueiredo RB, Langdon TG (2009) Int J Mater Res 100:843
4. Smirnova NA, Levit VI, Pilyugin VI, Kuznetsov RI, Davydova LS, Sazanova VA (1986) Fiz Met Metalloved 61:1170
5. Kondoh K, Aizawa T (2003) Mater Trans 44:1276
6. Segal VM (1995) Mater Sci Eng A197:157
7. Gottstein G, Al Samman T (2005) Mater Sci Forum 495–497:623
8. Vratna J, Strasky J, Janecek M, Kral R (2009) In: Kainer KU (ed) Magnesium. Wiley-VCH, Weinheim, p 331
9. Bohlen J, Yi S, Swiostek J, Letzig D, Brokmeier HG, Kainer KU (2005) Scripta Mater 53:259

10. Agnew SR, Mehrotra P, Lillo TM, Stoica GM, Liaw PK (2005) Mater Sci Eng A408:72
11. Estrin Y, Yi S, Brokmeier HG, Zuberova Z, Yoon SC, Kim HS, Hellmig RJ (2008) Int J Mater Res 99:50
12. Ion SE, Humphreys FJ, White SH (1982) Acta Mater 30:1909
13. Serebryany VN, Pozdnyakova NN, Kopylov VI, Dobatkin SV (2009) In: Kainer KU (ed) Magnesium. Wiley-VCH, Weinheim, p 181
14. Kang F, Liu JQ, Wang JT, Zhao X, Wu XL, Xia KN (2009) Int J Mater Res 100:1686
15. Al-Maharbi M, Foley DC, Karaman I, Hartwig KT, Kecskes LJ, Mathaudhu SN (2009) In: Kainer KU (ed) Magnesium. Wiley-VCH, Weinheim, p 321
16. Janecek M, Cizek J, Kuzel R, Vratna J (2010) J Alloys Compd (in press)